Robust Research of Power Oscillations Damping Controller for HVDC Inserted in Meshed AC Grids

Yankai Xing, Bogdan Marinescu, Florent Xavier

Robust Research of Power Oscillations Damping Controller for HVDC Inserted in Meshed AC Grids

Yankai Xing
Ecole Centrale de Nantes
LS2N-CNRS
Nantes, France
Yankai.Xing@ec-nantes.fr

Bogdan Marinescu
Ecole Centrale de Nantes
LS2N-CNRS
Nantes, France
Bogdan.Marinescu@ec-nantes.fr

Florent Xavier
RTE
R&D Division
Versailles, France
Florent.Xavier@rte-france.com

***Abstract*—This paper proposes a mixed sensitivity H_∞ controller to deal with damping of inter-area oscillations with a HVDC inserted in a meshed AC grid. In this case, inter-area modes may be at higher frequencies, close to other modes of the system. The classic tuning methods of standard (IEEE) power oscillations damping controller may not give satisfactory results for dynamics. A robust controller which is effective under different operating conditions is required. The controller design has been carried out based on the H_∞ mixed-sensitivity formulation in a LMI framework with pole-placement constraints. Investigations with nonlinear model of the system were done to settle and validate the approach. The efficiency and robustness of the proposed controller are tested and compared with a standard IEEE controller and a Linear Quadratic Gaussian one.**

***Index Terms*—Robustness, power system oscillations, HVDC, damping controller, inter-area modes**

I. Introduction

With the growth of the power grids, more and more High Voltage Direct Current (HVDC) transmission systems have been integrated in power grids. It is well known that inter-area oscillation modes can be damped by POD (Power Oscillation Damping) controllers of such lines which consist in supplementary (slower) control loops for active and reactive power modulation [1].

Recently, the interconnections in Europe have been reinforced by inserting HVDC lines (like, e.g., France-Spain and France-Italy links). As the European system is highly meshed, the inter-area modes impacted by such a HVDC link may be at higher frequencies - around 1Hz- than the well-known slowest inter-area modes which are around 0.2Hz. In this new frequency range, these inter-area modes are close to other modes of different nature which may be disturbed by the HVDC POD controller when synthesized by classic means [2]. This has been shown in our previous work [3] in which a solution to overcome this has been proposed. It is based on the use of an improved control model which captures all these dynamics and opens the way to advanced control. The preliminary Linear Quadratic (LQ) pole placement is replaced here by H_∞ to account for more robustness. This methodology, well-known in control systems to provide high robustness level (see, e.g., [4]) has already been used in power systems [5], [6], [7]. The main drawback of this approach or closely related H_2/LQ techniques [8], [9] is that the resulting control has the same order as the plant making it difficult to apply to large-scale power systems. However, this problem can be overcome by the use of low-order control model mentioned above and already used in [3].

H_∞ can be implemented using Linear Matrix Inequalities (LMI) [10], [11] which results in imposing poles to belong to specified regions of the complex plane. This provides us the possibility to directly specify and take into account in the controller synthesis the desired damping of the inter-area modes to be damped. This is the main performance specification for the HVDC POD control. The LMI framework is already used for damping specification in TCSC control [12].

Comparative studies are carried out on a realistic test grid as investigations between different approaches.

The paper is organized as follows: in Section II the modeling is given and the control problem is formulated. The basics and the design of the new control are given in Section III. The controller tuning is described in Section IV. Its application is discussed in Section V. Section VI is devoted to conclusions and perspectives of this work.

II. Problem formulation and modeling

Highly meshed transmission grids like the continental European one present inter-area modes at higher frequencies than the ones usually considered for damping control (around 0.2Hz in Europe). These modes are less spread (i.e., involve less number of generators and at lower geographic distances) and at frequencies around 1Hz. In this range of frequency other types of modes exist: local modes (electromechanical swings between close synchronous generators), electric coupling modes (related to purely electric coupling between distant devices) [7] or general electric modes linked to other electric phenomena. When such high frequency inter-area modes should be damped, specific cautions should be taken for the regulator to not disturb the other above mentioned modes in close frequency. Mainly, the *control model* (to take into account not only the modes to be damped but also the other modes) and *robustness* against neglected dynamics (which are at higher frequencies) should be improved.

TABLE I
THE LINEARIZED MODEL

No.	Mode	Damping ξ (%)	Freq. (Hz)	Mode shape (participation mag (%))		Residue	
				+	−	ABS MAG	Phase
1	-1.62+j8.19	19.5	1.30	GE_914 (100)	GE_913 (32.4)	0.0157	35.0
2	**-0.24+j5.53**	**4.5**	**0.88**	**GE_911 (100)**	**GE_917 (68.8)**	**0.0181**	**83.4**
3	-0.53+j5.29	10.1	0.84	GE_917 (100)	GE_918 (55.1)	0.0129	-56.2
4	-0.40+j4.79	8.3	0.76	GE_918 (44.3)	GE_912 (100)	0.0038	-33.3
5	-0.33+j3.29	10.1	0.52	GE_915 (100)	GE_918 (17.7)	0.0121	104.5
6	-18.83+j7.21	93.3	1.14	GE_921, GE_922 (100)	GE_923, GE_924 (74.1)	0.0034	14.5
7	-1.54+j6.55	22.9	1.04	GE_914 (100)	GE_911 (68.3)	0.0125	151.5
8	-19.32+j6.47	94.8	1.03	GE_921 (100)	GE_922 (37.6)	0.0117	118.9
9	-20.33+j4.86	97.2	0.77	GE_921, GE_922 (84.5)	GE_927 (100)	0.0026	-168.1
10	-18.72+j3.35	98.4	0.53	GE_913 (33.4)	GE_912 (100)	0.0072	136.1

A. Test system

The methodology proposed in this paper is tested on a HVDC line inserted in an AC grid composed by 19 generators. All generators are equipped with AVR (Automatic Voltage Regulator) and PSS (Power System Stabilizer). The full nonlinear model of this system, which is of order 724, is linearized to obtain the full linear model of the same order. This is a benchmark with former mentioned particularities.

Generally, it is desirable to have a high controllability and high observability of an oscillation mode to achieve high damping. In other words, only the modes of the grid which have highly residues in the transfers of the HVDC line can be damped by power modulation of the latter line. They are given in Table I for the considered test system. For each mode, the most participating machines are reported and categorized into two sets ('+' and '-') of generators oscillating against each other. The value of participation mag evaluates the contribution of each generator to the modes. For instance, 100% in the list means this generator is the most participating machine of this mode. For the inter-area modes these classes consist of machines for which the difference of the phase of right eigenvectors components related to the machine angle is close to $180°$. Notice that this table contains not only inter-area modes but also the local mode 8, which is due to the fact that generators GE921 and GE922 dominant in this mode are connected to the same bus. Mode 2 has very poor damping and it has thus to be considered in the control design process. This mode has two coherent most participating generators GE911 and GE917 which are swinging against each other. There are also several modes (highly damped (6 to 10) or poorly damped (1 to 5)) at frequencies close to the one of mode 2.

B. Control model

In the meshed grid context mentioned above, the control model based only on sensitivities of the modes to be damped against the gain of the controller usually used in POD controller synthesis [2] is no longer sufficient. To capture the dynamics mentioned above in frequencies close to the modes to be damped, two strategies are possible. First consists in starting from a full model of the power system and *reduce* it at a reasonable scale (about 10 state variables) for control by preserving dynamics of interest. This is very difficult for large-scale system and led us to a second approach based on *aggregation* of a transfer model around the modes of interest. If the open-loop transfer function of the full model is $H(s)$, the proposed control model consists in the low order transfer function $\tilde{H}(s)$ in (1) where the modes to be damped are $\Lambda = \{\lambda_1, ..., \lambda_l\}$ and r_k is the residue of mode λ_k.

$$\tilde{H}(s) = \frac{A(s)}{B(s)} + \frac{P(s)}{Q(s)} \quad (1)$$

$$\frac{A(s)}{B(s)} = \sum_{k=1}^{l} \left[\frac{r_k}{s-\lambda_k} + \frac{\bar{r}_k}{s-\bar{\lambda}_k} \right], \quad (2)$$

Polynomials $P(s)$ and $Q(s)$ are computed to minimize objective function (3) such that the reduced order model fits the full model system in the working frequency band. Notice that degree of $Q(s)$ is 7, so that the order of $\tilde{H}(s)$ is 12.

$$J = \sum_{\omega_\Lambda^- \le \omega_k \le \omega_\Lambda^+} [\alpha_k (A_k - |\tilde{H}(i\omega_k)|)^2 + \beta_k (\varphi_k - \arctan(\tilde{H}(i\omega_k)))^2] \quad (3)$$

where (A_k, ω_k) and (φ_k, ω_k) are points of the Bode plots of the transfer of the full model $H(s)$, ω_Λ^- and ω_Λ^+ give the range of working band. The weights α_k, β_k are used to give priority for the trade-off between phase and magnitude to eventually achieve the curve fitting in Bode plot at specific frequencies.

For the case tested here, Λ is composed by the first 5 modes in Table I, $\omega_\Lambda^- = 1.256$ rad/s and $\omega_\Lambda^+ = 13.8$ rad/s, α_k=1, β_k=1. The obtained results are shown in Fig. 1 where the reduced model fits the full model in the specified frequencies range.

C. Robustness

Robustness is the capability of a closed-loop to deal with mainly two classes of uncertainties of the model for which the control law is synthesized: variation of some of its parameters - called *parametric robustness* - and variation of the model structure itself - called *unstructured robustness*. In the case of power systems, in the first class we can include line trips, load or generation level evolution or other changes which preserve the system dimension but vary the operation point of the grid. For the HVDC case, change of the (amount and direction of)

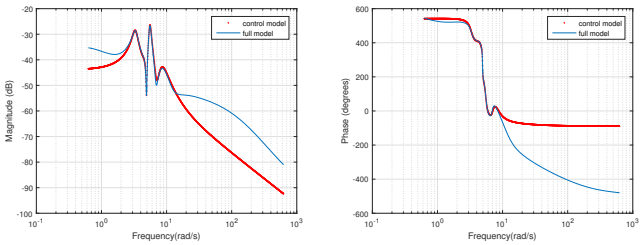

Fig. 1. Curve fitting of Bode plots of the full model and control model.

transferred active power is in this class. A control model is a reduced representation which focuses on dynamics of interest for the control. To be efficient and to lead to a small-size as the one proposed in section II-B controller and easy to synthesize, the latter should be of small-size. All neglected at this stage dynamics of the system enter in the class of unstructured robustness. The regulator should be such that the closed-loop provide high *attenuation* of such dynamics. In our case they may be due to more rapid (than inter-area modes) dynamics like the voltage/electric ones (voltage), speed/frequency disturbance (coming from load/production imbalance, oscillatory phenomena of other nature than inter-area modes, like, e.g., sub-synchronous oscillations, higher order harmonics, ...), noises (as disturbance signals generated by high-frequency exogenous signals) or effect of transmission delays in the regulation chain. Indeed, in the transfer formalism, a delay modeled by $e^{-\tau s}$ can be viewed as neglected high frequency dynamics if exponentials are approximated by rational transfer functions (i.e., Padé approximation).

Moreover, in the particular context considered here, as the modes to be damped are at higher frequencies and thus closer to the band of the unmodeled dynamics mentioned above, their attenuation is more difficult in the process of regulator synthesis.

The classic IEEE damping controller design synthesis [2] is simple but tends to lack of robustness even after careful tuning, which is due to that its phase compensation is settled down for a specific grid situation which may not be suitable for changed phase of residue of the mode. Also, robustness of the pole placement (done by LQG control) in the improved control framework reported in previous work [3] can be improved by the formalism below which has also the advantage to directly consider the damping target specification in the control synthesis.

III. New POD controller design

A. Basic of mixed sensitivity H_∞ control method (e.g., [4], [13])

H_∞ is one of the classic control formalism in which robustness specifications above can be met. It provides a multi-variable frequency loop-shaping using the H_∞ norm as quantitative measure of the attenuation. More precisely, the regulator is computed to minimize the input-output transfer of the modified plant in Fig. 2. The input signal to POD $\Delta\theta$ here is the angle difference between the HVDC terminals which is selected according [14], and Q_{pod} is the reactive modulation provided by the controller.

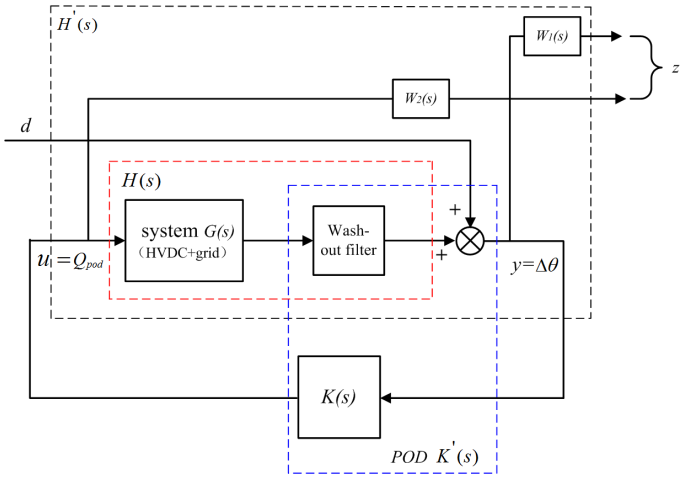

Fig. 2. Controller structure.

The input is disturbance d which stands for noise or the other dynamics mentioned above. The output z consists in the plant output y together with the control u in order to ensure minimum level control. The transfer function from d to y is the well-known sensitivity function *sensitivity function* $S(s) = (I + H(s)K(s)) - 1$. In order to minimize also the level of control, one has to consider

$$\left\| \begin{bmatrix} W_1(s)S(s) \\ W_2(s)KS(s) \end{bmatrix} \right\|_\infty < \gamma, \tag{4}$$

where $W_1(s)$ and $W_2(s)$ are frequency weights used to manage the trade-off robustness performance. They are low pass and respectively high pass filters and their tuning is given in Section IV. γ is the bound on H_∞ norm which guarantees the H_∞ performance.

Let

$$\begin{aligned} \dot{\chi} &= A_{cl}\chi + B_{cl}d \\ z &= C_{cl}\chi + D_{cl}d \end{aligned} \tag{5}$$

be a closed-loop state-space representation. Problem (4) can be converted into LMI sub-optimization problem given by (6) [10], [11].

$$\begin{bmatrix} A_{cl}^T X_{cl} + X_{cl}A_{cl}^T & B_{cl} & X_{cl}C_{cl}^T \\ B_{cl}^T & -I & D_{cl}^T \\ C_{cl}X_{cl} & D_{cl} & -\gamma^2 I \end{bmatrix} < 0 \tag{6}$$

B. Performance specification

Desired level of damping for the modes in Λ is equivalent to place the closed-loop poles in a sector region as in Fig. 3. This also can be formulated as an LMI optimization problem in Kronecker product form given by (7)

$$[\eta \otimes A_{cl}X_c + \eta^T \otimes X_c A_{cl}^T] < 0, \eta = \begin{bmatrix} \sin\frac{\theta}{2} & \cos\frac{\theta}{2} \\ -\cos\frac{\theta}{2} & \sin\frac{\theta}{2} \end{bmatrix} \tag{7}$$

θ is directly correlated with damping ratio $\xi = \cos\frac{\theta}{2}$ in left complex plane. In the case tested here $\xi_{desired} = 10\%$ for the modes in Table I, so $\theta = 168°$.

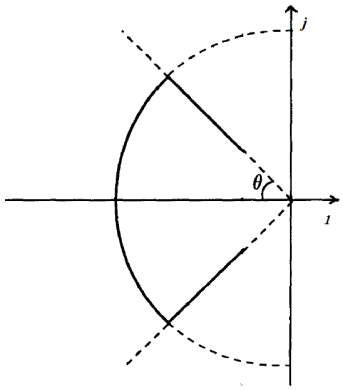

Fig. 3. LMI region.

According to [10], the jointly convexity of inequalities (6), (7) can be achieved by searching common solution, $X_{cl} = X_c = X_d$. These two inequalities also have non-linear terms $C_{cl}X_d$ and $A_{cl}X_d$ which cannot be solved by LMI optimization directly. To make it linear, a change of controller variables is necessary as shown in [10].

IV. Controller tuning

As for the classic POD synthesis, a wash-out filter is added to cancel the steady-state value of the measure and to focus the action of the controller to the frequency of the modes to be damped. So, the open-loop system used to calculate the controller $K(s)$ is $H(s)$, and final applied POD is $K'(s)$ in Fig. 2.

As mentioned in former section, $W_1(s)$ and $W_2(s)$ are weights used to shape the open-loop transfers with regulator. In this work $W_1(s)$ and $W_2(s)$ are chosen in the following classic form [13].

$$W_1(s) = \left(\frac{s/\sqrt[k]{M_s} + \omega_b}{s + \omega_b \sqrt[k]{\varepsilon}}\right)^k, W_2(s) = \left(\frac{s + \omega_{bc}/\sqrt[k]{M_n}}{\sqrt[k]{\varepsilon_1} s + \omega_{bc}}\right)^k \quad (8)$$

where ω_b, ω_{bc} is the bandwidth. M_s, M_n is the peak sensitivity. $\varepsilon, \varepsilon_1$ is the steady state error, and k is the order of the weighting function. For the example treated here $\varepsilon, \varepsilon_1 = 0.1$, $k = 1$, $\omega_b = 0.628$ rad/sec, $\omega_{bc} = 12.56$ rad/sec. The target damping is $\xi_{desired} = 10\%$ for the modes in Table I. The closed-loop damping ratios are shown in the first entries of Table II. Notice that with the classic controller it is not possible to provide a higher damping in this case for modes 2. Also, the damping of mode 4 is lower than in open-loop. With the advanced control, higher damping targets can be ensured. Synthesis was carried here at this almost common level of performances in order to facilitate comparison of robustness provided by each regulator.

TABLE II
Comparison damping

No.	ξ without POD (%)	ξ with classic POD (%)	ξ with LQG POD (%)	ξ with H_∞ POD (%)
1	19.5/19.8	30.5/24.43	21.7/20.66	20.29/21.36
2	4.5/5.04	6.1/5.76	10.9/7.86	11.67/9.87
3	10.1/9.65	12.0/11.91	14.9/11.53	12.33/13.89
4	8.3/8.28	8.1/8.07	11.4/9.31	12.41/10.86
5	10.1/10.85	12.4/12.30	13.6/13.57	14.97/12.51

V. Validation tests

In this section, performance is tested on the full nonlinear system and compared systematically for the 3 controllers: the classic POD, the LQG and the H_∞ ones. The tuning of classic and LQG PODs are detailed in [3].

A. Nominal behavior

Figure 4 shows the responses of the speed of generator GE911 to a 100ms duration short-circuit at the terminal bus of generator GE918. Notice that due to nonlinearities, each response curve captures the contribution of several modes mixed with nonlinear dynamics. Damping is improved with H_∞ POD particularly for the first two swings in which the nonlinearities of the system are the most present.

Consider the same duration short-circuit but at terminal of GE917. Figure 5 shows that the oscillations are damped with H_∞ POD better than the others. Notice that from the 6th swing till the end, mode 2 (the lowest damped in Table I) is the most observable in these responses.

Consider now the same duration short-circuit but at terminal of GE911. Figure 6 shows again better damping with H_∞ POD. However, let us recall that the damping target is the same and almost feasible for all the controller in order to facilitate robustness comparison. Indeed, larger differences will be put into evidence in the next section.

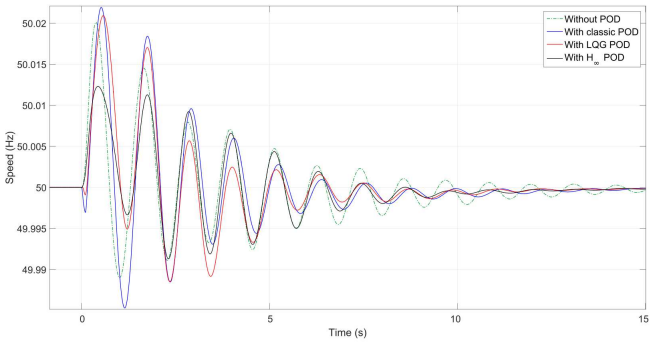

Fig. 4. Speed of GE911 in nominal case.

B. Robustness tests

1) Parametric robustness: The main variation of grid operating point in case of an HVDC comes from the modification of its active power flow. The extreme case is when not only the value of this flow is changed but also its direction. Here

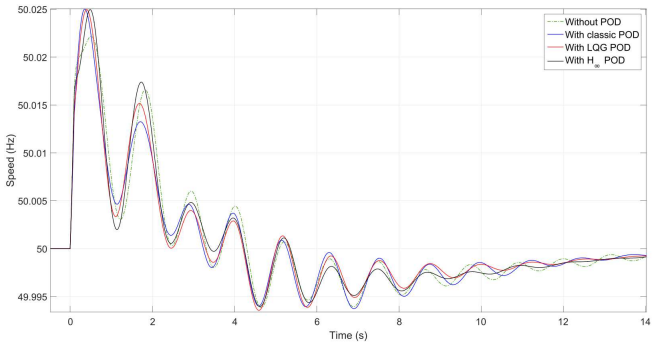

Fig. 5. Speed of GE912 in nominal case.

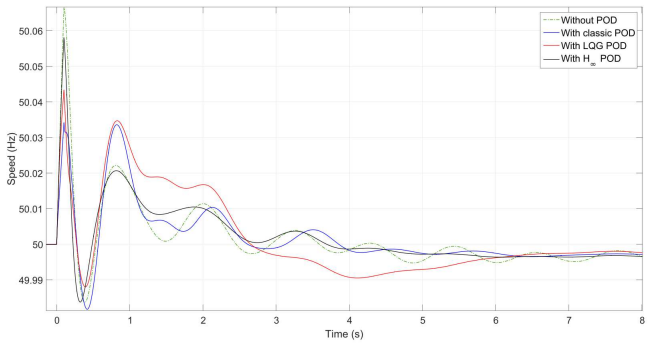

Fig. 6. Speed of GE914 in nominal case.

we consider the case where the regulators are synthesized on the nominal grid situation with active power flow $+800MW$ considered above. They are now tested on a new grid situation with power flow $-200MW$. The new damping ratios are shown in the second entries of Table II. The classic controller cannot ensure the damping objective. The most robust controller is the H_∞ one.

For nonlinear response, the same short-circuit as in the preceding section is considered. It is well known that LQ synthesis has less robustness than H_∞ approach [13], [4]. Nonlinear responses shown in Figure 7, 8, 9 confirm conclusions above.

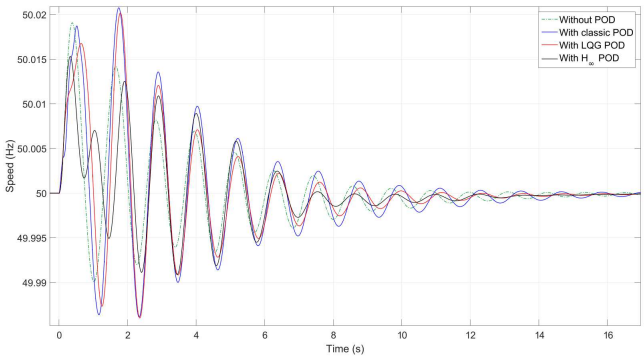

Fig. 7. Speed of GE911 for reversed power flow

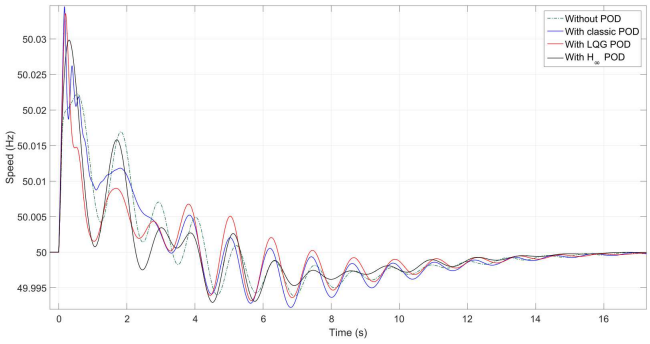

Fig. 8. Speed of GE912 for reversed power flow

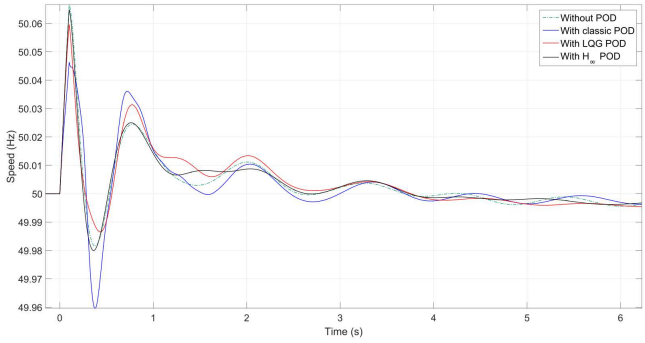

Fig. 9. Speed of GE914 for reversed power flow

2) Unstructured robustness and disturbance rejection: Consider disturbances d on the closed-loop in Fig. 2. From a *technological point of view*, this *output disturbance* can be due to meter disfunction (failure or bias) and/or measurement noise. From a *system point of view*, these signals may capture exogenous dynamics not taken into account in the nominal control model. This is classic for robust control [4]. As mentioned in Section II-C, for the case of the interconnected power systems, d may account for several neglected electric dynamics. As the control model is low frequency (focused on inter-area modes), such dynamics are of higher frequency. Here, they are considered at 10 Hz, generated as a step response of a second-order element tuned to this frequency. In other words,

$$d = \frac{\omega^2}{s^2 + 2\xi\omega s + \omega^2} u_d, \tag{9}$$

where $\omega = 62.8$ rad/sec, $\xi = 0.005$, u_d is a step of magnitude 0.005 pu.

The response with the full linear model, is shown in Fig 13. The nonlinear responses are shown in Fig 10, 11, 12. In both cases, the loop closed with the proposed H_∞ regulator is the most robust one.

VI. Conclusion and Perspectives

POD control of a HVDC link is addressed in the particular context where the link is inserted in a meshed AC grid. Interactions with other dynamics in the frequency range around

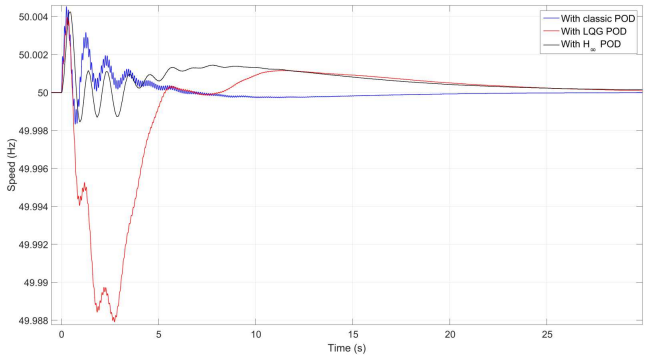

Fig. 10. Speed of GE911 for disturbance rejection

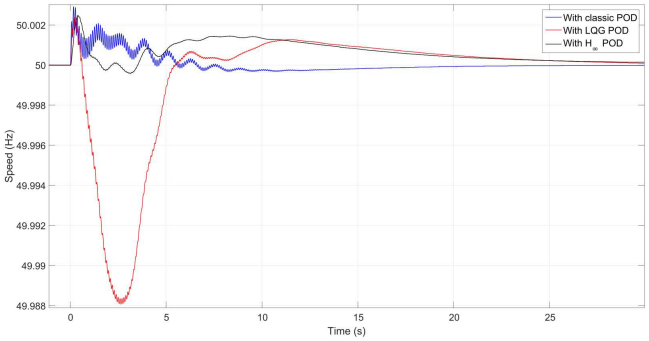

Fig. 11. Speed of GE912 for disturbance rejection

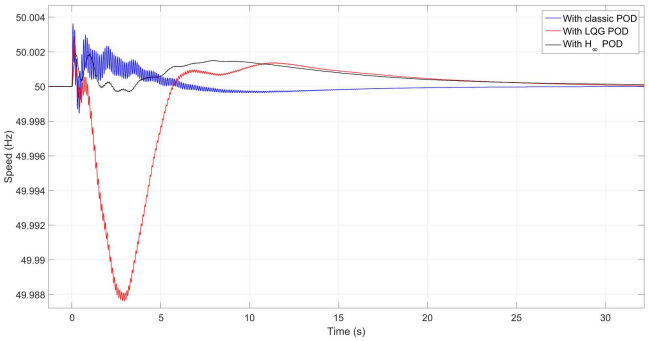

Fig. 12. Speed of GE914 for disturbance rejection

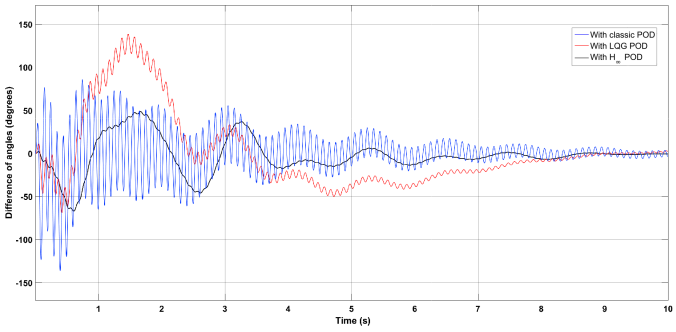

Fig. 13. Linear system output for disturbance rejection

1Hz are managed thanks to an enhanced control model which captures all these dynamics in a reasonable low order transfer function and to the use of robust H_∞ control. The latter allowed us to improve robustness against typical variations of the grid and un-modeled dynamics. In particular, good results are obtained in case of inversion of the direction of the active power flow and this avoids reconfiguration of the controller.

The implementation based on LMIs allowed us to directly and easily take into account in the synthesis of the regulator the desired damping for the modes as a sector constraint in the complex plane.

The approach will be extended to active power modulation. The coordination of the three modulations (active power and reactive power at both sides of the link) will be investigated. Also, other robust control methods (like fuzzy control, etc.) will be considered to further improve robustness.

ACKNOWLEDGMENT

The authors would like to thank China Scholarship Council (CSC) for the financial support to Yankai Xing.

REFERENCES

[1] H. F. Latorre, M. Ghandhari, and L. Söder, "Active and reactive power control of a vsc-hvdc," *Electric Power Systems Research*, vol. 78, no. 10, pp. 1756–1763, 2008.

[2] "IEEE recommended practice for excitation system models for power system stability studies (ieee std 421.5-2005)," *Energy Development and Power Generating Committee of the Power Engineering Society*, vol. 95, p. 96, 2005.

[3] Y. Xing, B. Marinescu, M. Belhocine, and F. Xavier, "Power oscillations damping controller for hvdc inserted in meshed ac grids," in *Innovative Smart Grid Technologies Conference Europe (ISGT-Europe), 2018 IEEE PES*. IEEE, 2018.

[4] S. Skogestad and I. Postlethwaite, *Multivariable feedback control: analysis and design*. Wiley New-York, 2007.

[5] K. Vance, A. Pal, and J. S. Thorp, "A robust control technique for damping inter-area oscillations," in *Power and Energy Conference at Illinois (PECI), 2012 IEEE*. IEEE, 2012, pp. 1–8.

[6] B. Chaudhuri and B. C. Pal, "Robust damping of multiple swing modes employing global stabilizing signals with a tcsc," *IEEE Transactions on Power Systems*, vol. 19, no. 1, pp. 499–506, 2004.

[7] L. Arioua and B. Marinescu, "Robust grid-oriented control of high voltage dc links embedded in an ac transmission system," *International Journal of Robust and Nonlinear Control*, vol. 26, no. 9, pp. 1944–1961, 2016.

[8] R. Preece, J. V. Milanovic, A. M. Almutairi, and O. Marjanovic, "Damping of inter-area oscillations in mixed ac/dc networks using wams based supplementary controller," *IEEE Transactions on Power Systems*, vol. 28, no. 2, pp. 1160–1169, 2013.

[9] A. C. Zolotas, P. Korba, B. Chaudhuri, and I. M. Jaimoukha, "H2 lmi-based robust control for damping oscillations in power systems," in *System of Systems Engineering, 2007. SoSE'07. IEEE International Conference on*. IEEE, 2007, pp. 1–8.

[10] M. Chilali and P. Gahinet, "H-infinity design with pole placement constraints: an lmi approach," *IEEE Transactions on automatic control*, vol. 41, no. 3, pp. 358–367, 1996.

[11] C. Scherer, P. Gahinet, and M. Chilali, "Multiobjective output-feedback control via lmi optimization," *IEEE Transactions on automatic control*, vol. 42, no. 7, pp. 896–911, 1997.

[12] D. Mondal, A. Sengupta, and A. Chakrabarti, "Robust control of inter-area oscillations in a multimachine network employing lmi based wide area tcsc controller," *Electrical and Electronic Engineering*, vol. 2, no. 2, pp. 23–30, 2012.

[13] K. Zhou and J. C. Doyle, *Essentials of robust control*. Prentice hall Upper Saddle River, NJ, 1998, vol. 104.

[14] M. Belhocine, B. Marinescu, and F. Xavier, "Input signal and model structure analysis for the hvdc link pod control," in *PowerTech, 2017 IEEE Manchester*. IEEE, 2017, pp. 1–6.